Proceedings of the 36th Chinese Control Conference
July 26-28, 2017, Dalian, China

On Existence Conditions of A Class of Continuous Curvature Paths

Jin Dai[1,2], Yebin Wang[1]

1. Mitsubishi Electric Research Laboratories, Cambridge, MA 02139, USA (e-mail:{jdai,yebinwang}@merl.com).

2. Department of Electrical Engineering, University of Notre Dame, Notre Dame, IN 46556, USA (e-mail: jdai1@nd.edu).

Abstract: Local steering, which constructs a kinematically or dynamically feasible path between two configurations, is a core component of various path planning methods. This paper investigates the continuous curvature (CC) steering for car-like robots subject to constraints on velocity, curvature and derivative of the curvature. Based on the $\mu-$tangency conditions in [9], we establish existence conditions for a class of CC paths which admit the same driving patterns as the Reeds-Shepp paths [6]. These conditions allow efficient implementation of the CC steering, which enables real-time CC path planning. The feasibility and computation efficiency of the resultant CC steering are validated by numerical simulations.

Key Words: Path planning, nonholonomic dynamics, car-like robots, continuous-curvature paths

1 Introduction

Path planning problem of mobile robots has been extensively investigated during the past few decades, with the consideration of various kinematic, dynamic and environmental constraints [1–3]. A vast majority of research efforts have been devoted to path planning of robots with nonholonomic dynamics [4–7] and particularly car-like robots, due to the broad applications of car-like platforms [8].

Pioneering work [5, 6] has shown that shortest length paths, also known as Reeds-Shepp (RS) paths, are sequential composition of line segments and tangential circular arcs of the minimum turning radius. Nevertheless, the curvature along these optimal paths is discontinuous. This is undesirable in practice, since a mobile robot has to stop and perform stationary steering, leading to unnecessary time delay and extra wearing of tires [8, 9].

Many contributions have been made to constructing optimal continuous curvature (CC) [9] paths for car-like robots. Work [10–12] established the existence of optimal CC paths, which are composed of clothid curves and line segments; however, it is also shown that the line segment involves infinite chattering. This discouraging discovery motivates the study of finding computationally efficient sub-optimal CC paths. For instance, work [13] planed CC paths based on Bézier curve fitting; nonetheless, sub-optimality was not extensively studied therein. Work [14] developed a numerically efficient planning scheme, which is applicable to forward-moving robots.

This paper considers schemes to enable real-time computation of sub-optimal CC paths for car-like robots with curvature and its time derivative bounded. The sub-optimal CC paths admit the same driving patterns as the RS paths, and thus can be viewed as a generalization of the RS paths. Based on the $\mu-$tangency conditions [9, 12], we establish existence conditions of the sub-optimal CC paths. The existence conditions can be used to determine whether a sub-optimal CC path with a specific driving pattern exists, and how to construct efficiently.

The remainder of this paper is organized as follows. Section 2 presents the kinematic model of a car-like robot and formulates the optimal path planning problem. In Section 3, we review the RS paths as well as clothoid curves and $\mu-$tangency conditions. The clothoid curves and $\mu-$tangency conditions are further utilized in Section 4 to derive existence conditions of CC paths. Section 5 compares RS steering and the proposed CC steering by simulation. Concluding remarks are presented in Section 6.

2 Preliminaries

Besides stating the continuous curvature (CC) path planning problem, this section overviews classes and patterns of Reeds-Shepp (RS) paths, clothoid turns, and $\mu-$tangenecy conditions. Readers are referred to [6, 9] for details.

2.1 Kinematic Model of Car-like Robots

Fig. 1 illustrates the car-like robot, which is equipped with a front-fixed steering wheel and fixed parallel rear wheels. The point R is located at the mid of the rear wheels. The pose of the robot is uniquely described by a triple (x, y, θ) where (x, y) represent the coordinates of R in the global frame and θ is the orientation angle of the robot with respect to the positive x-axis of the global frame. The robot has a wheelbase b, and a steering angle ϕ.

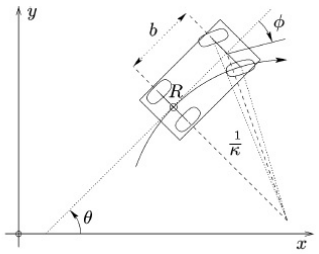

Fig. 1: A car-like robot with reference point R [9].

The kinematic model of the car-like robot is given by

$$\begin{pmatrix} \dot{x} \\ \dot{y} \\ \dot{\theta} \\ \dot{\kappa} \end{pmatrix} = \begin{pmatrix} \cos\theta \\ \sin\theta \\ \kappa \\ 0 \end{pmatrix} v + \begin{pmatrix} 0 \\ 0 \\ 0 \\ 1 \end{pmatrix} \sigma, \tag{1}$$

where the curvature κ is an extra configuration parameter in

addition to (x, y, θ). The control inputs of system (1) are $u = (v, \sigma)$, where v is the driving velocity of the rear wheels and σ the *steering rate*. The relationship between ϕ, κ and σ is established as follows:

$$\kappa = \frac{\tan\phi}{b}, \sigma = \dot{\kappa} = \frac{\dot{\phi}}{b\cos^2\phi}.$$

Assume that both forward and backward motions are allowed for the robot and the driving velocity is bounded, whereas the angle of the steering wheel is subject to mechanical constraints, i.e.,

$$|v| \leq v_{max}, |\phi| \leq \phi_{max}, |\kappa| \leq \kappa_{max} := \frac{\tan\phi_{max}}{b}. \quad (2)$$

The steering rate σ is also assumed to be bounded, i.e.,

$$|\sigma| \leq \sigma_{max}. \quad (3)$$

Thus, the set of admissible control inputs is defined by

$$\mathcal{U} = \{u \in \mathfrak{U} : u(t) \in U, t \in [0, T_f]\}, \quad (4)$$

where $\mathfrak{U}$ is the set of all measurable functions defined over $[0, T_f]$, and $U := [-v_{max}, v_{max}] \times [-\sigma_{max}, \sigma_{max}]$.

2.2 Optimal Path Planning Problem

Given an initial configuration $q_0 = (x_0, y_0, \theta_0, \kappa_0)$, a final configuration $q_f = (x_f, y_f, \theta_f, \kappa_f)$ and the model (1) with constraints (2) (3), we aim to find a feasible and optimal path between q_0 and q_f.By normalizing the velocity of the robot, i.e., $|v| = 1$, planning the optimal (shortest) feasible path is equivalent to solving the following optimal control problem.

Problem 1 (Optimal Path Planning)**.** *Given a robot with dynamics (1) and the cost functional*

$$J(u) = \int_0^{T_f} dt = T_f, \quad (5)$$

determine the optimal control input $u^* \in \mathcal{U}$ with $u^* : [0, T_f] \mapsto U$ and the associated optimal state trajectory $\mathbf{q}^* : [0, T_f] \mapsto \mathbb{R}^2 \times \mathbb{S}^1 \times \mathbb{R}$, such that

1) *Boundary conditions $\mathbf{q}^*(0) = q_0 = (x_0, y_0, \theta_0, \kappa_0)$, and $\mathbf{q}^*(T_f) = q_f = (x_f, y_f, \theta_f, \kappa_f)$;*
2) *Feasibility $\forall t \in [0, T_f]$, $\mathbf{q}^*(t) \in \mathbb{R}^2 \times \mathbb{S}^1 \times [-\kappa_{max}, \kappa_{max}]$;*
3) *Optimality The optimal control u^* minimizes the cost functional $J(u)$.*

Similar to [9], we assume that q_0, q_f have null-curvature configurations, i.e., $\kappa_0 = \kappa_f = 0$. Extension to connecting non-zero curvature configurations can be achieved. Without loss of generality, we further assume $q_0 = (0, 0, 0, 0)$.

2.3 Reeds-Shepp Paths

As shown in [6], RS paths can be categorized into 12 classes, and admit a total of 48 patterns. All classes and patterns are summarized in Table 1, where C stands for a circular curve and S stands for a line segment; while L and R specify left and right turns with $+$ or $-$ denoting forward or backward motion, respectively. In addition, the subscripts denote the (absolute) angular value of a certain circular arc and $|$ represents a cusp occurring in a path.

Table 1: Reeds-Shepp Classes of Paths

Classes	Patterns
$CSC-1$	L+S+L+, L-S-L-, R+S+R+, R-S-R-
$CSC-2$	L+S+R+, L-S-R-, R+S+L+, R-S-L-
$C\|C\|C$	L+R-L+, L-R+L-, R+L-R+, R-L+R-
$C\|CC$	L+R-L-, L-R+L+, R+L-R-, R-L+R+
$CC\|C$	L+R+L-, L-R-L+, R+L+R-, R-L-R+
$CC_u\|C_uC$	L+R+L-R-, L-R-L+R+, R+L+R-L-, R-L-R+L+
$C\|C_uC_u\|C$	L+R-L-R+, L-R+L+R-, R+L-R-L+, R-L+R+L-
$C\|C_{\frac{\pi}{2}}SC-1$	L+R-S-R-, L-R+S+R+, R+L-S-L-, R-L+S+L+
$C\|C_{\frac{\pi}{2}}SC-2$	L+R-S-L-, L-R+S+L+, R+L-S-R-, R-L+S+R+
$CSC_{\frac{\pi}{2}}\|C-1$	L+S+L+R-, L-S-L-R+, R+S+R+L-, R-S-R-L+
$CSC_{\frac{\pi}{2}}\|C-2$	L+S+R+L-, L-S-R-L+, R+S+L+R-, R-S-L-R+
$C\|C_{\frac{\pi}{2}}SC_{\frac{\pi}{2}}\|C$	L+R-S-L-R+, L-R+S+L+R-, R+L-S-R-L+, R-L+S+R+L-

2.4 Clothoid Turns

We utilizes the same clothoids [9] to ensure the continuity of curvature along sub-optimal CC paths. A clothoid is a curve whose curvature is an affine function of the arc length s, i.e., $\kappa(s) = \kappa(0) + \sigma s$, where σ is termed as the *sharpness* of the clothoid. A clothoid turn (CT) from $q_0 = (x_0, y_0, \theta_0, 0)$ to an endpoint $q_g(x_g, y_g, \theta_g, 0)$ is characterized by its *deflection* $\delta = (\theta_g - \theta_0) \mod 2\pi$. Without loss of generality, we consider the robot (1) moving along a forward and left clothoid turn with deflection $0 \leq \delta < 2\pi$ from $q_0 = (0, 0, 0, 0)$. Let $\delta_c = \kappa_{max}^2/(2\sigma_{max})$. For the case where $2\delta_c \leq \delta \leq 2\delta_c + \pi$, the robot first follows a clothoid with σ_{max} until the curvature $\kappa = \kappa_{max}$. The configuration q of the robot at distance s from the initial configuration is given by

$$q(s) = \begin{pmatrix} x(s) \\ y(s) \\ \theta(s) \\ \kappa(s) \end{pmatrix} = \begin{pmatrix} \sqrt{\pi/\sigma_{max}} C_f\left(s/\sqrt{\pi/\sigma_{max}}\right) \\ \sqrt{\pi/\sigma_{max}} S_f\left(s/\sqrt{\pi/\sigma_{max}}\right) \\ \sigma_{max} s^2/2 \\ \sigma_{max} s \end{pmatrix},$$

where $C_f(s) = \int_0^s \cos\frac{\pi}{2}\tau^2 d\tau$ and $S_f(s) = \int_0^s \sin\frac{\pi}{2}\tau^2 d\tau$ are the Fresnel cosine and sine integrals, respectively. This clothoid ends at

$$q_1 := \begin{pmatrix} x_1 \\ y_1 \\ \theta_1 \\ \kappa_1 \end{pmatrix} = \begin{pmatrix} \sqrt{\pi/\sigma_{max}} C_f\left(\sqrt{\kappa_{max}^2/(\pi\sigma_{max})}\right) \\ \sqrt{\pi/\sigma_{max}} S_f\left(\sqrt{\kappa_{max}^2/(\pi\sigma_{max})}\right) \\ \delta_c \\ \kappa_{max} \end{pmatrix}.$$

From q_1, the robot enters a circular arc of radius κ_{max}^{-1} and of an angular value $\theta = \delta - 2\delta_c$. The center Ω of the underlying circle is

$$\begin{pmatrix} x_\Omega \\ y_\Omega \end{pmatrix} = \begin{pmatrix} x_1 - \kappa_{max}^{-1}\sin\theta_1 \\ y_1 + \kappa_{max}^{-1}\cos\theta_1 \end{pmatrix}.$$

The circular arc ends at $q_2 = (x_2, y_2, \delta - \delta_c, \kappa_{max})$ for some x_2 and y_2. We define radius R_Ω and angle μ between the orientation of q_i and the tangent to the circle of center Ω (henceforth called a *CC Circle* C_l^+ of a forward left turn), as follows,

$$R_\Omega = \sqrt{x_\Omega^2 + y_\Omega^2}, \mu = \arctan(x_\Omega/y_\Omega).$$

After the robot leaves the circular arc, it follows another clothoid with sharpness $-\sigma_{max}$ until the curvature reduces to zero. The clothoid turn CT of deflection $2\delta_c \leq \delta \leq 2\delta_c + \pi$ is then formed by: (i) a clothoid starting at q_0 with sharpness κ_{max} and of length $\kappa_{max}/\sigma_{max}$; (ii) a circular arc of radius κ_{max}^{-1} and of angle $\delta - 2\delta_c$; (iii) a second clothoid with sharpness $-\kappa_{max}$ and of length $\kappa_{max}/\sigma_{max}$.

For the case where $0 < \delta < 2\delta_c$, a clothoid of sharpness $\sigma \leq \sigma_{max}$ and a symmetric clothoid arc of sharpness $-\sigma$ are used to reach the deflection. To purse computationally convenient path planning in the following sections, we require that (x_g, y_g) be also located at $C_l^+(q_0)$. Toward this end, the desired sharpness σ is given by [9]

$$\sigma = \frac{\pi \left[\cos(\delta/2) C_f(\sqrt{\delta/\pi}) + \sin(\delta/2) S_f(\sqrt{\delta/\pi})\right]^2}{R_\Omega^2 \sin^2(\delta/2 + \mu)}$$

and the arc length of each clothoid arc is $\sqrt{\delta/\sigma}$.

Finally, for the case $\delta = 0$, the clothoid turn reduces to a straight line segment of length $2R_\Omega \sin\mu$, so as to ensure that q_g belongs to $C_l^+(q_0)$. It is worth pointing out that although backward motion is allowed for the robot (1), we require that the direction of motion remain unchanged within a single clothoid turn, for the sake of clarity of presentation. This additional restriction eliminates the clothoid turn case in [9] where $2\delta_c + \pi \leq \delta < 2\pi$.

2.5 μ-Tangency Conditions

The μ-tangency conditions between clothoid turns and line segments are first presented. Recall that in the RS path planning paradigm, a connection between a circular arc and a line segment is needed at a configuration q if and only if the line segment is tangent to the circle associated with q. For CC paths, the line segment must cross the CC circle associated with the configuration q and make an angle of μ. The idea is illustrated in Fig. 2.

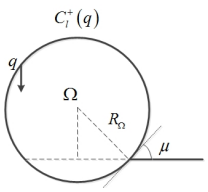

Fig. 2: μ-tangency between line segments and CC circles.

The $\mu-$tangency conditions between clothoid turns are derived as follows. We take a path of the form $L+R+$ that connects two configurations q_1 and q_2 as an example to explain μ-tangency conditions when the direction of motion does not change. As shown in Fig. 3, the μ-tangency conditions suggest that the CC circle $C_l^+(q_1)$ be tangent to $C_r^-(q_2)$. The intermediate configuration q_3 serves not only the final configuration of the left clothoid turn from q_1 but the initial configuration of the right clothoid turn ending at q_2. Specifically, angles between the orientation of q_3 and tangent vectors of both $C_l^+(q_1)$ and $C_r^-(q_2)$ are μ. The corresponding μ-tangency condition is

$$L(\Omega_1\Omega_2) = 2R_\Omega,$$

where $L(\Omega_1\Omega_2)$ is the distance between the centers of the two CC circles.

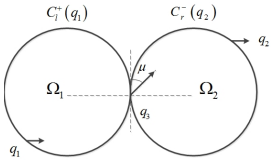

Fig. 3: μ-tangency between CC circles (with no cusp).

Moreover, we take a path of the form $L+R-$ that connects two configurations q_1 and q_2 as an example to explain μ-tangency conditions when the direction of motion changes. This case is illustrated by Fig. 4, where a cusp emerges on the path. Let q_3 be the configuration of the cusp, and q_3 must be located at one of the intersection points of the CC circles $C_l^+(q_1)$ and $C_r^+(q_2)$. The μ-tangency condition requires that the orientation of q_3 makes an angle of μ with respect to both CC circles. This type of μ-tangency condition validates if and only if both of the following conditions hold simultaneously:

1) $L(\Omega_1\Omega_2) = 2R_\Omega \cos\mu$;
2) The orientation of q_3 is vertical to $\Omega_1\Omega_2$.

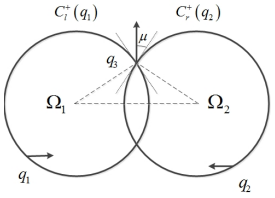

Fig. 4: μ-tangency between CC circles (with a cusp).

3 Main Results

This section derives existence conditions of the CC paths that admit the RS path classes in Table. 1. Due to space limitation, we only consider the CC paths starting with the word $L+$ that connect the null-curvature initial and final configurations $q_0 = (0,0,0,0)$ and $q_f = (x_f, y_f, \theta_f, 0)$ (henceforth deemed as *canonical* paths). Since the $CSC-1$ and $CSC-2$ classes have been investigated in [9] and the two $CSC_{\frac{\pi}{2}}|C$ classes can be constructed similarly to the $C|C_{\frac{\pi}{2}}SC$ classes, we present here the existence conditions for 8 classes: $C|C|C$, $C|CC$, $CC|C$, $CC_u|C_uC$, $C|C_uC_u|C$, $C|C_{\frac{\pi}{2}}SC-1$, $C|C_{\frac{\pi}{2}}SC-2$ and $C|C_{\frac{\pi}{2}}SC_{\frac{\pi}{2}}|C$. We introduce the validity of paths to simplify computation.

Definition 1 (Valid Paths)**.** *A canonical continuous-curvature path is said to be valid if: (i) for all clothoid turns that are admitted by the path, $0 \leq \delta < 2\delta_c + \pi$ holds for a positive deflection and $-2\delta_c - \pi \leq \delta < 0$ for a negative deflection; (ii) the total length of the path $L > 0$.*

3.1 $C|C|C$ Paths

The $L+R-L+$ path suggests that the two forward and left clothoid turns be connected by a right and backward clothoid turn. The geometric scenario is demonstrated in

Fig. 5. The CC circles $C_l^+(q_0)$ for q_0 and $C_l^-(q_f)$ for q_f are employed to characterize the final configuration q_1 of the first left clothoid turn, and the initial configuration q_2 of the second left clothoid turn.

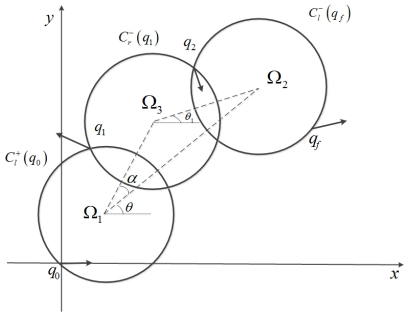

Fig. 5: Geometric setup of $C|C|C$ paths

The CC circle $C_r^-(q_1)$ must coincide with $C_r^+(q_2)$. Let Ω_3 denote the center of the third CC circle, and α denote the angle between $\Omega_1\Omega_2$ and $\Omega_1\Omega_3$. The μ-tangency conditions between $C_l^+(q_0)$ and $C_r^-(q_1)$ and between $C_r^-(q_1)$ and $C_l^-(q_f)$ suggest

$$L(\Omega_1\Omega_3) = L(\Omega_2\Omega_3) = 2R_\Omega \cos\mu. \tag{6}$$

Applying law of cosines in the triangle $\Omega_1\Omega_2\Omega_3$ yields

$$\begin{aligned}\cos\alpha &= \frac{L^2(\Omega_1\Omega_2) + (2R_\Omega\cos\mu)^2 - (2R_\Omega\cos\mu)^2}{2\cdot L(\Omega_1\Omega_2)\cdot 2R_\Omega\cos\mu} \\ &= \frac{L(\Omega_1\Omega_2)}{4R_\Omega\cos\mu}.\end{aligned} \tag{7}$$

Therefore the coordinate of Ω_3 can be given by

$$\Omega_3 = \begin{pmatrix} x_{\Omega_3} \\ y_{\Omega_3}\end{pmatrix} = \begin{pmatrix} x_{\Omega_1} + 2R_\Omega\cos\mu\cos(\theta+\alpha) \\ y_{\Omega_1} + 2R_\Omega\cos\mu\sin(\theta+\alpha)\end{pmatrix}. \tag{8}$$

Let θ_1 denote the angle between $\Omega_2\Omega_3$ and the positive x-axis. The path $L+R-L+$ is therefore composed of

1) A left clothoid turn CT_1: the μ-tangency between $C_l^+(q_0)$ and $C_r^-(q_1)$ asserts that the orientation of q_1 is $\theta+\alpha+\frac{\pi}{2}$, which is exactly the deflection δ_1;
2) A backward and right clothoid turn CT_2: since the orientation of q_2 is $\theta_1 - \frac{\pi}{2}$ according to the μ-tangency between $C_l^-(q_f)$ and $C_r^-(q_1)$, the deflection of CT_2 is $\delta_2 = \theta_1 - \theta - \alpha - \pi$;
3) A second left clothoid turn CT_3 with deflection $\delta_3 = \theta_f - \theta_1 + \frac{\pi}{2}$.

Existence conditions: (i) δ_1, δ_2 and δ_3 all satisfy Definition 1; (ii) the triangle $\Omega_1\Omega_2\Omega_3$ should be valid, i.e., $0 \le L(\Omega_1\Omega_2) \le 4R_\Omega\cos\mu$.

3.2 $C|CC$ Paths

The $C|CC$ path, $L+R-L-$, can be processed in the same way as the $C|C|C$ path. As shown in Fig. 6, after computing the center Ω_1 of $C_l^+(q_0)$ and Ω_2 of $C_l^+(q_f)$, we aim to determine the intermediate configurations q_1, q_2, and the center, denoted as Ω_3, of the CC circle $C_r^-(q_1)$.

The μ-tangency between $C_l^+(q_0)$ and $C_r^-(q_1)$, and between $C_r^-(q_1)$ and $C_l^+(q_f)$, implies

$$L(\Omega_1\Omega_3) = 2R_\Omega\cos\mu, L(\Omega_2\Omega_3) = 2R_\Omega.$$

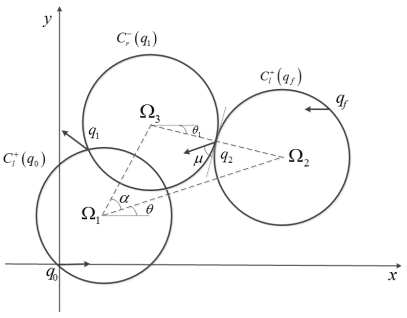

Fig. 6: Geometric setup of $C|CC$ paths

Let α denote the angle between $\Omega_1\Omega_2$ and $\Omega_1\Omega_3$. The law of cosines suggests that, in the triangle $\Omega_1\Omega_2\Omega_3$,

$$\begin{aligned}\cos\alpha &= \frac{L^2(\Omega_1\Omega_2) + (2R_\Omega\cos\mu)^2 - (2R_\Omega)^2}{2\cdot L(\Omega_1\Omega_2)\cdot 2R_\Omega\cos\mu} \\ &= \frac{L^2(\Omega_1\Omega_2) - (2R_\Omega\sin\mu)^2}{4L(\Omega_1\Omega_2)R_\Omega\cos\mu}.\end{aligned} \tag{9}$$

The coordinates of Ω_3 can be represented by (8), with α computed by (9). Let θ_1 denote the angle between $\Omega_2\Omega_3$ and the positive x-axis. Thus the path $L+R-L-$ consists of

1) A left clothoid turn CT_1 with deflection $\delta_1 = \theta+\alpha+\frac{\pi}{2}$;
2) A backward and right clothoid turn CT_2: since the orientation of q_2 is $\theta_1 - \frac{\pi}{2} - \mu$, the deflection of CT_2 is $\delta_2 = \theta_1 - \theta - \alpha - \mu - \pi$;
3) A backward and left clothoid turn CT_3 with deflection, $\delta_2 = \theta_f - \theta_1 + \frac{\pi}{2} + \mu$, which guarantees that the final configuration of CT_3 is identical to q_f.

Existence conditions: (i) δ_1, δ_2 and δ_3 satisfy Definition 1; (ii) the triangle $\Omega_1\Omega_2\Omega_3$ should be valid, i.e.,

$$2R_\Omega(1-\cos\mu) \le L(\Omega_1\Omega_2) \le 2R_\Omega(1+\cos\mu).$$

3.3 $CC|C$ Paths

The geometric setup is illustrated in Fig. 7, where the center of $C_l^+(q_0)$ is Ω_1 and the center of $C_l^+(q_f)$ is Ω_2. Let

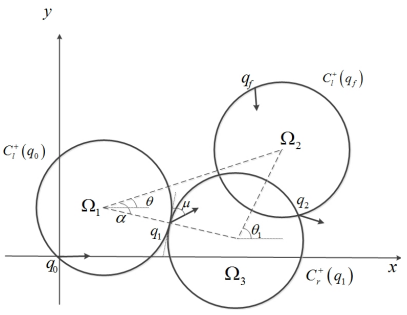

Fig. 7: Geometric setup of $CC|C$ paths

q_1 and q_2 be the two intermediate configurations. To determine the center Ω_3 of the CC circle $C_r^-(q_1)$, we apply law of cosines in the triangle $\Omega_1\Omega_3\Omega_2$ to obtain the angle α:

$$\begin{aligned}\cos\alpha &= \frac{L^2(\Omega_1\Omega_2) + (2R_\Omega)^2 - (2R_\Omega\cos\mu)^2}{2\cdot L(\Omega_1\Omega_2)\cdot 2R_\Omega} \\ &= \frac{L^2(\Omega_1\Omega_2) + (2R_\Omega\sin\mu)^2}{4L(\Omega_1\Omega_2)R_\Omega},\end{aligned} \tag{10}$$

which yields the coordinate of Ω_3

$$\Omega_3 = \begin{pmatrix} x_{\Omega_3} \\ y_{\Omega_3} \end{pmatrix} = \begin{pmatrix} x_{\Omega_1} + 2R_\Omega \cos(\theta - \alpha) \\ y_{\Omega_1} + 2R_\Omega \sin(\theta - \alpha) \end{pmatrix}. \quad (11)$$

Let θ_1 denote the angle between $\Omega_2\Omega_3$ and the positive x-axis. The path $L + R + L-$ is the concatenation of

1) A left clothoid turn CT_1: the μ-tangency between $C_l^+(q_0)$ and $C_r^+(q_1)$ implies that the orientation of q_1 is $\theta - \alpha + \frac{\pi}{2} - \mu$, i.e, $\delta_1 = \theta - \alpha + \frac{\pi}{2} - \mu$;
2) A forward and right clothoid turn CT_2: since the μ-tangency between $C_r^+(q_1)$ and $C_l^+(q_f)$ implies that the orientation of q_2 is $\theta_1 - \frac{\pi}{2}$, thus $\delta_2 = \theta_1 - \theta + \alpha - \mu - \pi$;
3) A backward and left clothoid turn CT_3 with deflection $\delta_3 = \theta_f - \theta_1 + \frac{\pi}{2}$.

Existence conditions: (i) δ_1, δ_2 and δ_3 all satisfy Definition 1; (ii) the triangle $\Omega_1\Omega_3\Omega_2$ be valid, i.e.,

$$2R_\Omega(1 - \cos\mu) \le L(\Omega_1\Omega_2) \le 2R_\Omega(1 + \cos\mu). \quad (12)$$

3.4 $CC_u|C_uC$ Paths

Taking into account the symmetry of $CC_u|C_uC$ and the $\mu-$tangency, one can derive total four feasible geometric setups of $CC_u|C_uC$ paths. Due to space limitation, Fig. 8 illustrates one feasible geometric setup to solve the $CC_u|C_uC$ path. One can see that, the computation of such a $CC_u|C_uC$ is reduced to the determination of the intermediate configurations q_1, q_2, q_3 or centers of the associated CC circles.

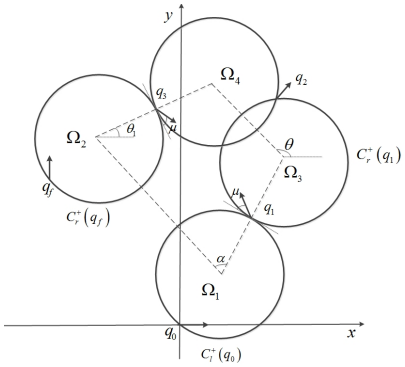

Fig. 8: Geometric setup of $CC_u|C_uC$ paths

Let Ω_1 and Ω_2 denote the center of the CC circles $C_l^+(q_0)$ and $C_r^+(q_f)$, respectively; and let θ denote the angle between $\Omega_1\Omega_2$ and the positive x-axis. We let the centers of $C_r^+(q_1)$ and $C_l^-(q_2)$ be Ω_3 and Ω_4, respectively. The μ-tangency conditions imply that

$$\begin{aligned} L(\Omega_1\Omega_3) &= L(\Omega_2\Omega_4) = 2R_\Omega \cos\mu \\ L(\Omega_3\Omega_4) &= 2R_\Omega. \end{aligned} \quad (13)$$

To determine the coordinates of Ω_3 and Ω_4, we exploit the symmetry of $CC_u|C_uC$ to establish that $\Omega_3\Omega_4$ must be *parallel* to $\Omega_1\Omega_2$. This fact implies that $\Omega_1\Omega_3\Omega_4\Omega_2$ is an isosceles trapezoid. Let α denote the angle between $\Omega_1\Omega_2$ and $\Omega_1\Omega_3$, a straightforward geometric analysis implies that

$$\begin{aligned} \cos\alpha &= \frac{\frac{1}{2}(L(\Omega_1\Omega_2) - L(\Omega_3\Omega_4))}{L(\Omega_1\Omega_3)} \\ &= \frac{L(\Omega_1\Omega_2) - 2R_\Omega\cos\mu}{4R_\Omega}. \end{aligned} \quad (14)$$

Based on (14) and Fig. 8, the coordinates of Ω_3 and Ω_4 are respectively given by

$$\begin{aligned} \Omega_3 &= \begin{pmatrix} x_{\Omega_3} \\ y_{\Omega_3} \end{pmatrix} = \begin{pmatrix} x_{\Omega_1} + 2R_\Omega\cos(\theta - \alpha) \\ y_{\Omega_1} + 2R_\Omega\sin(\theta - \alpha) \end{pmatrix} \\ \Omega_4 &= \begin{pmatrix} x_{\Omega_4} \\ y_{\Omega_4} \end{pmatrix} = \begin{pmatrix} x_{\Omega_3} + 2R_\Omega\cos\mu\cos\theta \\ y_{\Omega_3} + 2R_\Omega\cos\mu\sin\theta \end{pmatrix}. \end{aligned} \quad (15)$$

Let θ_1 represent the angle between $\Omega_2\Omega_4$ and the positive x-axis, the $L + R_u + L_u - R-$ path can then be formed by sequentially composing

1) A forward and left clothoid turn CT_1: the μ-tangency condition between $C_l^+(q_0)$ and $C_r^+(q_1)$ implies that the orientation of q_1 is $\theta - \alpha - \mu + \frac{\pi}{2}$, thus the deflection of CT_1 is $\delta_1 = \theta - \alpha - \mu + \frac{\pi}{2}$;
2) A forward and right clothoid turn CT_2: the μ-tangency condition between $C_r^+(q_1)$ and $C_l^-(q_2)$ implies that the orientation of q_2 is $\theta - \frac{\pi}{2}$, thus the deflection of CT_2 is $u = \alpha + \mu - \pi$;
3) A backward and left clothoid turn CT_3 with the same deflection $u = \alpha + \mu - \pi$;
4) A backward and right clothoid turn CT_4: the μ-tangency condition between $C_l^-(q_2)$ and $C_r^+(q_f)$ implies that the orientation of q_3 is $\theta_1 - \frac{\pi}{2} + \mu$, thus the deflection of CT_4 is $\delta_2 = \theta_f - \theta_1 - \mu + \frac{\pi}{2}$.

Existence conditions: (i) δ_1, δ_2 and u all satisfy Definition 1; (ii) the angle α is well defined, thus

$$2R_\Omega \le L(\Omega_1\Omega_2) \le 2R_\Omega\cos\mu + 4R_\Omega.$$

3.5 $C|C_uC_u|C$ Paths

To appropriately generate the $C|C_uC_u|C$ path, namely $L + R_u - L_u - R+$, we need to determine three intermediate configurations q_1, q_2, q_3, as shown in Fig. 9. Denote Ω_1 and

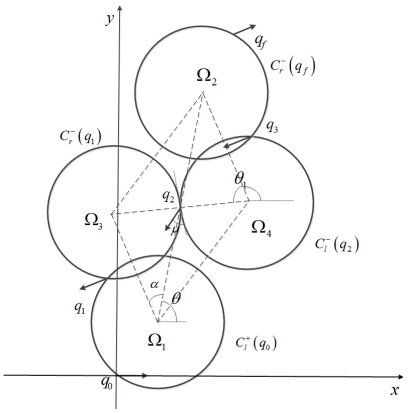

Fig. 9: Geometric setup of $C|C_uC_u|C$ paths

Ω_2 the centers of the CC circles $C_l^+(q_0)$ and $C_r^-(q_f)$ associated with q_0 and q_f, respectively. Let θ be the angle between $\Omega_1\Omega_2$ and the positive x-axis. As shown in Fig. 9, Ω_3 and Ω_4 are the centers of the CC circles $C_r^-(q_1)$ and $C_l^-(q_2)$, respectively. The μ-tangency between $C_l^+(q_0)$ and $C_r^-(q_1)$, and between $C_l^-(q_2)$ and $C_r^-(q_f)$ implies that

$$L(\Omega_1\Omega_3) = L(\Omega_2\Omega_4) = 2R_\Omega\cos\mu.$$

The μ-tangency between $C_r^-(q_1)$ and $C_l^-(q_2)$ implies that

$$L(\Omega_3\Omega_4) = 2R_\Omega.$$

Proposition 1. *$\Omega_1\Omega_3$ is parallel to $\Omega_2\Omega_4$.*

Proof. Let θ_1 denote the angle between $\Omega_1\Omega_3$ and the positive x-axis, and let θ_2 denote the angle between $\Omega_4\Omega_2$ and the positive x-axis. The μ-tangency between $C_l^+(q_0)$ and $C_r^-(q_1)$ enforces the orientation of q_1 to be $\theta_1 + \frac{\pi}{2}$. Thus, after a backward and right clothoid turn with deflection u, the orientation of q_2 is $\theta_1 + \frac{\pi}{2} + u$ and similarly, the orientation of q_3 is $\theta_1 + \frac{\pi}{2} + u - u = \theta_1 + \frac{\pi}{2}$.

On the other hand, serving as the initial configuration of the final backward and right clothoid turn connecting q_3 and q_f, the μ-tangency between $C_l^-(q_2)$ and $C_r^-(q_f)$ assures the orientation of q_3 to be $\theta_2 + \frac{\pi}{2}$. Thus $\theta_1 = \theta_2$, which suffices to prove that $\Omega_1\Omega_3$ is parallel to $\Omega_2\Omega_4$. □

It follows immediately from Proposition 1 that $\Omega_1\Omega_4$-$\Omega_2\Omega_3$ is a parallelogram. Let α denote the angle between $\Omega_1\Omega_2$ and $\Omega_1\Omega_3$. Applying law of cosines in the triangle $\Omega_1 q_2 \Omega_3$ yields

$$\begin{aligned}\cos\alpha &= \frac{(\frac{1}{2}L(\Omega_1\Omega_2))^2 + L^2(\Omega_1\Omega_3)) - (\frac{1}{2}L(\Omega_3\Omega_4))^2}{2L(\Omega_1\Omega_3)\frac{1}{2}L(\Omega_1\Omega_2)} \\ &= \frac{\frac{1}{4}L^2(\Omega_1\Omega_2) + (2R_\Omega\cos\mu)^2 - R_\Omega^2}{2L(\Omega_1\Omega_2)R_\Omega\cos\mu}.\end{aligned}$$

The coordinates of Ω_3 and Ω_4 are obtained as:

$$\begin{aligned}\Omega_3 &= \begin{pmatrix} x_{\Omega_3} \\ y_{\Omega_3}\end{pmatrix} = \begin{pmatrix} x_{\Omega_1} + 2R_\Omega\cos\mu\cos(\theta+\alpha) \\ y_{\Omega_1} + 2R_\Omega\cos\mu\sin(\theta+\alpha)\end{pmatrix} \\ \Omega_4 &= \begin{pmatrix} x_{\Omega_4} \\ y_{\Omega_4}\end{pmatrix} = \begin{pmatrix} x_{\Omega_1} + x_{\Omega_2} - x_{\Omega_3} \\ y_{\Omega_1} + y_{\Omega_2} - y_{\Omega_3}\end{pmatrix}.\end{aligned} \tag{16}$$

As illustrated in Fig. 9 and Proposition 1, the path $L + R_u - L_u - R+$ is the sequential concatenation of

1) A left clothoid turn CT_1 with deflection $\delta_1 = \theta + \alpha + \frac{\pi}{2}$;
2) A backward and right clothoid turn CT_2 with deflection $u = \theta_1 - \theta - \alpha - \mu$;
3) A backward and left clothoid turn CT_3 with deflection $-u$.
4) A forward and right clothoid turn CT_4 with deflection $\delta_2 = \theta_f - \theta - \alpha - \frac{\pi}{2}$.

Existence conditions: (i) δ_1, δ_2 and u all satisfy Definition 1; (ii) the triangle $\Omega_1 q_2 \Omega_3$ be valid, i.e.,

$$|2R_\Omega - 4R_\Omega\cos\mu| \le L(\Omega_1\Omega_2) \le 2R_\Omega + 4R_\Omega\cos\mu.$$

3.6 $C|C_{\frac{\pi}{2}}SC-1$ Paths

To build up an $L+R-S-R-$ path that connects q_0 and q_f, we need to determine the intermediate configurations q_1, q_2 and q_3, which represents the initial configuration of the first backward right clothoid turn, the line segment and the second backward right clothoid turn, respectively. Toward this end, we use the CC circles $C_l^+(q_0)$ with center Ω_1 for q_0 and $C_t^+(q_f)$ with center Ω_2 for q_f. Let θ denote the angle between $\Omega_1\Omega_2$ and the positive x-axis. The geometric setup is shown in Fig. 10, where Ω_3 is the the center of the CC circle $C_r^-(q_1)$. The coordinates of Ω_3 can be determined according to the following proposition.

Proposition 2. *Ω_1, Ω_2 and Ω_3 are collinear.*

Proof. Let θ_1 denote the angle between $\Omega_1\Omega_3$ and the positive x-axis, and θ_2 the angle between $\Omega_3\Omega_2$ and the positive

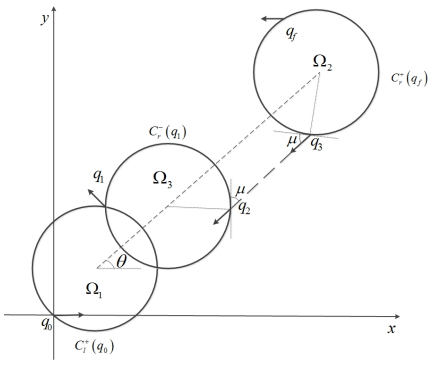

Fig. 10: Geometric setup of $C|CSC-1$ paths

x-axis. The μ-tangency between $C_l^+(q_0)$ and $C_r^-(q_1)$ indicates that the orientation of q_1 is $\theta_1 + \frac{\pi}{2}$, thus the orientation of q_2 is $\theta_1 + \pi$. On the other hand, based on the μ-tangency between q_2q_3 and $C_t^+(q_f)$, q_2q_3 is parallel to $\Omega_2\Omega_3$, and the orientation of q_3 is $\theta_2 + \pi$, thus we have

$$\theta_1 + \pi = \theta_2 + \pi \Rightarrow \theta_1 = \theta_2,$$

indicating the collinearity of Ω_1, Ω_2 and Ω_3. □

Given Proposition 2, the $L+R-S-R-$ path can be computed immediately

1) A forward and left clothoid turn CT_1 with deflection $\delta_1 = \theta + \frac{\pi}{2}$;
2) A backward and right clothoid turn CT_2 with deflection $\delta_2 = \frac{\pi}{2}$
3) A straight line segment q_2q_3 of length

$$\begin{aligned}L(q_2q_3) &= L(\Omega_2\Omega_3) - 2R_\Omega\sin\mu \\ &= L(\Omega_1\Omega_2) - 2R_\Omega\cos\mu - 2R_\Omega\sin\mu;\end{aligned}$$

4) A second backward and right clothoid turn CT_3 with deflection $\delta_3 = \theta_f - \theta - \pi$.

Existence conditions: (i) δ_1, δ_2 and δ_3 satisfies Definition 1; (ii) $L(q_2q_3) \ge 0$, that is

$$L(\Omega_1\Omega_2) \ge 2R_\Omega(\cos\mu + \sin\mu).$$

3.7 $C|C_{\frac{\pi}{2}}SC-2$ Paths

The construction of $C|CSC-2$ class of the CC paths requires a slightly different geometric analysis procedure. The $L+R-S-L-$ path involves two CC circle $C_l^+(q_0)$ and $C_l^+(q_f)$, with centers Ω_1 and Ω_2, respectively. Let θ denote the angle between $\Omega_1\Omega_2$ and the positive x-axis. The geometric setting is illustrated in Fig. 11.

Let q_1, q_2 and q_3 represent the initial configuration of the first backward right clothoid turn, the line segment and the second backward right clothoid turn, respectively. Let Ω_3 be the center of the CC circle $C_r^-(q_1)$, and α the angle between $\Omega_1\Omega_3$ and $\Omega_1\Omega_2$. We extend $\Omega_1\Omega_3$ to Ω_0 such that $\Omega_2\Omega_0$ is perpendicular to $\Omega_1\Omega_0$. Let $\Omega_3 A$ be perpendicular to q_2q_3, and B the intersecting point of $\Omega_2\Omega_0$ and q_2q_3. Based on the μ-tangency between $C_l^+(q_0)$ and $C_r^-(q_1)$, the orientation of both q_2 and q_3 is $\theta + \alpha + \pi$, which implies that q_2q_3 is parallel to $\Omega_1\Omega_0$ and is perpendicular to $\Omega_0\Omega_2$, indicating

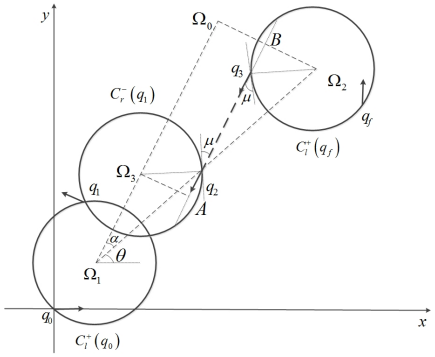

Fig. 11: Geometric setup of $C|CSC-2$ paths

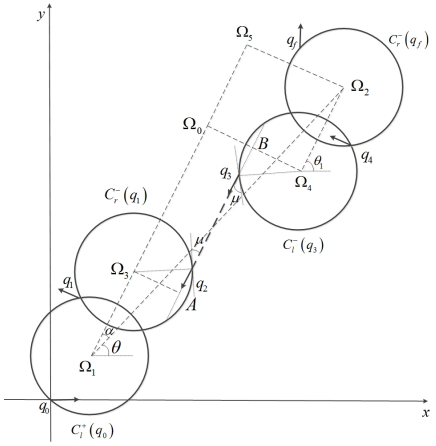

Fig. 12: Geometric setup of $C|CSC|C$ paths

that $\Omega_3AB\Omega_0$ is a rectangle. The μ-tangency between q_2q_3 and $C_r^-(q_1)$, and between q_2q_3 and $C_l^+(q_f)$ suggests

$$L(\Omega_3A) = L(\Omega_2B) = L(\Omega_0B) = R_\Omega \cos\mu,$$

which implies that, in the right triangle $\Omega_0\Omega_1\Omega_2$,

$$\sin\alpha = \frac{L(\Omega_0\Omega_2)}{L(\Omega_1\Omega_2)} = \frac{2R_\Omega\cos\mu}{L(\Omega_1\Omega_2)}. \tag{17}$$

It immediately follows from (17) that the $L+R-S-L-$ CC path consists of

1) A forward and left clothoid turn CT_1 with deflection $\delta_1 = \theta + \alpha + \frac{\pi}{2}$;
2) A backward and right clothoid turn CT_2 with deflection $\delta_2 = \frac{\pi}{2}$
3) A straight line segment q_2q_3 of length

$$\begin{aligned} L(q_2q_3) &= L(AB) - 2R_\Omega\sin\mu \\ &= L(\Omega_3\Omega_0) - 2R_\Omega\sin\mu \\ &= L(\Omega_1\Omega_2)\cos\alpha - 2R_\Omega\cos\mu - 2R_\Omega\sin\mu; \end{aligned}$$

4) A second backward and right clothoid turn CT_3 with deflection $\delta_3 = \theta_f - \theta - \pi$.

Existence conditions: (i) δ_1, δ_2 and δ_3 satisfies Definition 1; (ii) $L(q_2q_3) \geq 0$, that is

$$\begin{aligned} &L(\Omega_1\Omega_2) \geq 2R_\Omega\cos\mu \\ &\sqrt{L^2(\Omega_1\Omega_2) - (2R_\Omega\cos\mu)^2} \geq 2R_\Omega(\cos\mu + \sin\mu). \end{aligned}$$

3.8 $C|C_{\frac{\pi}{2}}SC_{\frac{\pi}{2}}|C$ Paths

Finally, we derive existence conditions of the $C|CSC|C$ path, $L+R-S-L-R+$. Let $C_l^+(q_0)$ and $C_r^-(q_f)$ be the CC circles associated with q_0 and q_f, whose centers are Ω_1 and Ω_2, respectively. Let θ denote the angle between $\Omega_1\Omega_2$ and the positive x-axis. The geometric setup of $L+R-S-L-R+$ is depicted in Fig. 12.

As shown in Fig. 12, to appropriately determine the intermediate configurations q_1, q_2, q_3 and q_4, one needs to take advantage of the CC circles $C_r^-(q_1)$ and $C_l^-(q_3)$, whose centers are Ω_3 and Ω_4, respectively.

Proposition 3. *$\Omega_1\Omega_3$ is parallel to $\Omega_4\Omega_2$.*

Proof. Let θ_1 and θ_2 be the angle between $\Omega_1\Omega_3$, $\Omega_4\Omega_2$ and the positive x-axis, respectively. The μ-tangency between $C_l^+(q_0)$ and $C_r^-(q_1)$ enforces the orientation of q_1 to be $\theta_1 + \frac{\pi}{2}$, and the $\frac{\pi}{2}$ deflection of the backward and right clothoid turn suggests the orientation of q_2 and q_3 be $\theta_1 + \pi$. Therefore, after the backward and left clothoid turn with deflection $-\frac{\pi}{2}$, the orientation of q_4 shall be $\theta_1 + \frac{\pi}{2}$. On the other hand, the μ-tangency between $C_l^-(q_3)$ and $C_r^-(q_f)$ implies that the orientation of q_4 is $\theta_2 + \frac{\pi}{2}$. Thus $\theta_1 = \theta_2$, i.e., $\Omega_1\Omega_3$ is parallel to $\Omega_4\Omega_2$. □

Let $\Omega_4\Omega_0$ be perpendicular to $\Omega_1\Omega_3$. Since $q_0q_1q_2q_3q_4$ forms a $L+R-S-L-$ path from q_0 to q_4, it follows from the previous reasoning that $L(\Omega_4\Omega_0) = 2R_\Omega\cos\mu$. Moreover, let Ω_5 be a point on the straight line $\Omega_1\Omega_3$ such that $\Omega_2\Omega_5$ is perpendicular to $\Omega_1\Omega_5$. From Proposition 3, $\Omega_4\Omega_2 = 2R_\Omega\cos\mu$ and is parallel to $\Omega_1\Omega_5$, making $\Omega_0\Omega_4\Omega_2\Omega_5$ a square. Therefore, the auxillary angle α can be determined in the right triangle $\Omega_1\Omega_2\Omega_5$:

$$\sin\alpha = \frac{L(\Omega_2\Omega_5)}{L(\Omega_1\Omega_2)} = \frac{2R_\Omega\cos\mu}{L(\Omega_1\Omega_2)}. \tag{18}$$

It follows immediately from (18) that the $L+R-S-L-R+$ CC path is formed by

1) A forward and left clothoid turn CT_1 with deflection $\delta_1 = \theta + \alpha + \frac{\pi}{2}$;
2) A backward and right clothoid turn CT_2 with deflection $\delta_2 = \frac{\pi}{2}$;
3) A backward line segment q_2q_3 of length

$$\begin{aligned} L(q_2q_3) &= L(\Omega_3\Omega_0) - 2R_\Omega\sin\mu \\ &= \sqrt{L^2(\Omega_1\Omega_2) - (2R_\Omega\cos\mu)^2} \\ &\quad - 4R_\Omega\cos\mu - 2R_\Omega\sin\mu \end{aligned}$$

4) A backward and left clothoid turn CT_3 with deflection $\delta_3 = -\frac{\pi}{2}$;
5) A forward and right clothoid turn CT_4 with deflection $\delta_3 = \theta_f - \theta - \alpha - \frac{\pi}{2}$.

Existence conditions: (i) δ_1 and δ_4 satisfies Definition 1; (ii) $L(q_2q_3) \geq 0$, that is

$$\begin{aligned} &L(\Omega_1\Omega_2) \geq 2R_\Omega\cos\mu, \\ &\sqrt{L^2(\Omega_1\Omega_2) - (2R_\Omega\cos\mu)^2} \geq 4R_\Omega\cos\mu + 2R_\Omega\sin\mu, \end{aligned}$$

4 Simulation

The effectiveness of existence conditions and the resultant CC steering algorithm are validated through simulation. We check the feasibility of constructing an RS and a CC path connecting $q_0 = (0, 0, 0, 0)$ and 1000 different q_f's, where each q_f is randomly generated in $q_f \in [-4, 4] \times [-4, 4] \times (-\pi, \pi) \times \{0\}$. Table 2 shows that the resultant CC steering algorithm can find feasible CC paths for all cases. In terms of computation efficiency, the construction of the shortest CC path takes about 20 times longer than that of the RS path.

Table 2: RS vs. CC Feasibility

Paths	RS Paths	CC Paths	Ratio
Feasible Classes (Avg.)	24.3200	8.6280	2.8187
Planning Time (Avg.)	0.5579 ms	10.4220 ms	25.7414
Computation Time(Avg.)	0.1260 ms	2.8193 ms	21.9234

Next, we show that, as the σ_{max} increases, CC paths converge to corresponding RS paths. This is illustrated by designing an $L + R - L-$ path from $(0, 0, 0, 0)$ to $(-2, -2, -0, 0)$ with σ_{max} varies from 0.5 to 50. As shown in Figs. 13-14, the length of the CC path converges to the length of the RS path, as σ_{max} increases, while the path itself converges to the RS path.

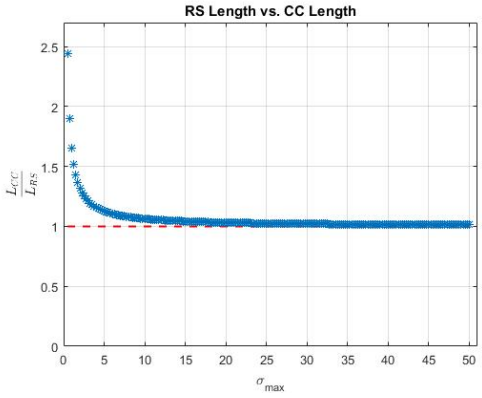

Fig. 13: Reeds-Shepp and continuous-curvature paths

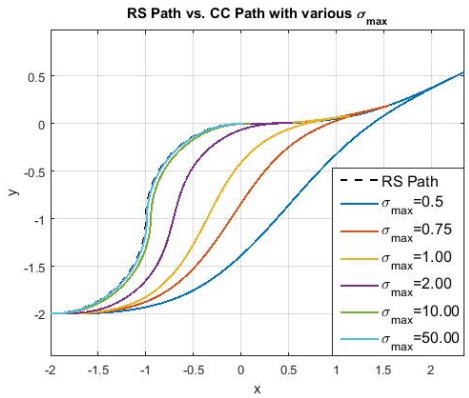

Fig. 14: Reeds-Shepp and continuous-curvature paths

5 Conclusion

This paper explored methods to efficiently construct a class of sub-optimal continuous curvature paths for car-like robots. Based on the established $\mu-$tangency, existence conditions of continuous-curvature paths, having the same patterns as the Reeds-Shepp paths, were derived via geometric analysis. The effectiveness of the proposed approach was demonstrated by simulation.

References

[1] H. Choset, K. M. Lynch, S. Hutchinson, G. Kantor, W. Burgard, L. E. Kavraki, and S. Thrun, *Principles of Robot Motion: Theory, Algorithms, and Implementations*, Boston: MIT Press, 2005.

[2] S. M. LaValle, *Planning Algorithms*, Cambridge, U.K.: Cambridge Univ. Press, 2006.

[3] G. E. Fainekos, A. Girard, H. Kress-Gazit, and G. J. Pappas, "Temporal logic motion planning for dynamic robots," *Automatica*, 45(2): 343–352, 2009.

[4] P. R. Giordano, M. Vendittelli, J-P. Laumond, and P. Souéres, "Nonholonomic distance to polygonal obstacles for a car-like robot of polygonal shape," *IEEE Trans. Robot.*, 22(5): 1040–1047, 2006.

[5] L. E. Dubins, "On curves of minimal length with a constraint on average curvature, and with prescribed initial and terminal positions and tangents," *American Journal of Mathematics*, 79(3): 497–516, 1957.

[6] J. A. Reeds and L. A. Shepp, "Optimal paths for a car that goes both forwards and backwards," *Pacific Journal of Mathematics*, 145(2): 367–393, 1990.

[7] J-P. Laumond, P. E. Jacobs, M. Taix and R. M. Murray, "A motion planner for nonholonomic mobile robots," *IEEE Trans. Robot. Automat.*, 10(5): 577–593, 1994.

[8] H. Vorobieva, S. Glaser, N. Minoiu-Enache and S. Mammar, "Automatic parallel parking in tiny spots: path planning and control," *IEEE Trans. Intell. Transp. Syst.*, 16(1): 396–410, 2015.

[9] T. Fraichard and A. Scheuer, "From Reeds and Shepp's to continuous-curvature paths," *IEEE Trans. Robot.*, 20(6): 1025–1035, 2004.

[10] J-D. Boissonnat, A. Cerezo and J. Leblond, "A note on shortest paths in the plane subject to a constraint on the derivative of the curvature," *Research Report*, RR-2160, INRIA, France, 1994.

[11] H. J. Sussmann, "The Markov-Dubins problem with angular acceleration control," *Proc. of the 1997 ICRA*, 2639–2643, 1997.

[12] A. Scheuer and C. Laugier, "Planning sub-optimal and continuous-curvature paths for car-like robots," *Proc. of the 1998 IROS*, 25–31, 1998.

[13] K. Yang and S. Sukkarieh, "An analytical continuous-curvature path-smoothing algorithm," *IEEE Trans. Robot.*, 26(3): 561-568, 2010.

[14] E. Bakolas and P. Tsiotras, "On the generation of nearly optimal, planar paths of bounded curvature and bounded curvature gradient," *Proc. of the 2009 ACC*, 385–390, 2009.